Abstract: **One of the major challenges in harnessing wind energy is to extract maximum power from intermittent generation of wind farms as wind power generation strongly depends on wind speed variation. In grid connected mode, a DFIG is expected to operate at optimum speed to deliver maximum output power in the grid while the voltage, frequency and harmonic regulations need to be fulfilled. Among different maximum power point tracking (MPPT) algorithms, the Hill Climb Search (HCS) method is preferred because of its simple implementation and turbine parameter-independent scheme. Since the conventional HCS algorithm has few drawbacks such as power fluctuation and speed-efficiency trade-off, a new adaptive step size based HCS controller is proposed in this paper to mitigate its deficiencies by incorporating wind speed measurement in the controller. The function-based adaptive control scheme evaluates the step size by the variation of the wind speed and extracted power range. Thus the scheme tracks the optimum rotor speed under turbulent condition. The adaptive MPPT controller along with PI controlled doubly fed induction generator (DFIG) can effectively track the maximum power generated from a wind turbine with less perturbation. The overall system is simulated and the experimentation is done with a low-power DFIG prototype in the laboratory. The designed controller shows improved performance over conventional HCS MPPT controller and the outcomes of the testing are found quite satisfactory when compared to the simulation results.**

Keywords: **On-line tuning, ANFIS control, Doubly fed induction generator, Wind energy conversion system, Power control.**

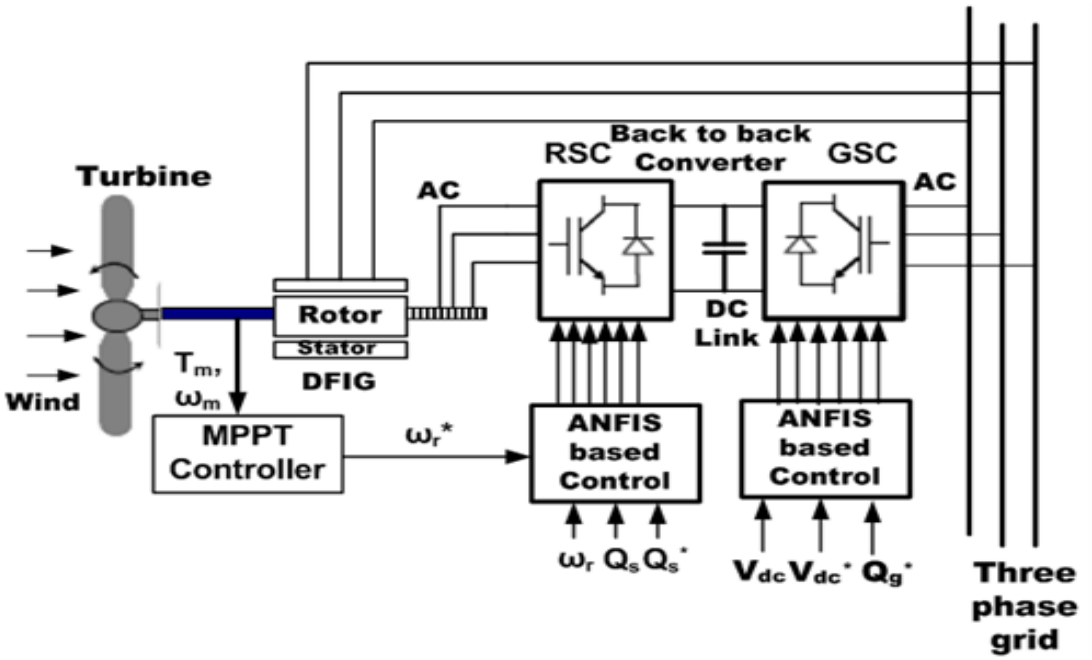

Fig.1. Full configuration of the proposed ANFIS controller based DFIG-WECS

1. Introduction

The use of doubly-fed induction generator has recently gained vast popularity in grid connected wind energy conversion system because of its economic operation, ability to regulate in sub-synchronous or super-synchronous speed and decoupled control of active and reactive power. Among the major challenges of WECS, controlled extraction of power from intermittent generation and supervision on nonlinear system dynamics of DFIG-WECS are of critical importance. Various adaptive and intelligent control techniques have been adopted by researchers to regulated the real and reactive power in DFIG driven WECS [1-5]. Vector control associated with PI controllers has been widely recognized and applied in industry for reliable power regulation of DFIG. However, the performance of the vector control based system depends on the parameter tuning of the PI controllers, voltage condition at the grid end, randomness in wind speed, etc. Furthermore, the performance of the fixed-gain PI controller deteriorates with the variation in machine parameters due to the change in temperature, magnetic saturation and machine-aging. Therefore, the researchers have focused more on sophisticated solutions for WECS control, such as backstepping based nonlinear control [6], fuzzy logic control [7], sliding mode control [8] etc. Nonlinear control techniques are dependent on the model equations and suffer from the problem of gained efficiency vs complexity trade-off. The major drawback of the reported fuzzy inference system is that it is completely based on the knowledge and experience of the designer [9]. The current components of the generators are prone to the chattering effect in sliding mode control of DFIG-WECS. On the other hand, intelligent control algorithms such as neural network (NN), neuro-fuzzy control (NFC), adaptive network-based fuzzy inference system (ANFIS), genetic algorithm, particle swarm optimization, artificial bee colony algorithm, grey wolf optimization have not been thoroughly investigated yet for wind energy conversion system. ANFIS provides adaptability on choosing the membership functions and fast convergence due to its hybrid learning. Moreover, ANFIS architecture has the distinguishing feature of modelling a highly nonlinear system, as it combines the competence of fuzzy reasoning in handling uncertainties and learning aptitude of neural network from complex system [10]. Therefore, it has been chosen as the control algorithm for grid-connected wind power generation in this paper.

2. Proposed Configuration of the System

In the proposed configuration, the DFIG is mechanically coupled with the turbine to transform the mechanical energy into electrical energy. A back-to-back converter is implanted to perform independent control of DC-link voltage and decoupled control of real and reactive power. Separate control circuits are required to regulate the grid-side converter (GSC) and rotor side converter (RSC) as shown in Fig. 1. Adaptive neuro-fuzzy scheme with on-line tuning feature is implemented to design the proposed controllers. The turbine, DFIG and grid parameters are shown in Table 1.

2.1 ANFIS Network

The controller for the converters is designed by utilizing fuzzy logic and artificial neural network algorithms. ANFIS can be considered as an intelligent and powerful processing tool for pattern recognition and controller design because it combines the advantages of both the fuzzy logic and neural network algorithms. The parameters associated with the membership functions are updated by gradient descent algorithm. When the gradient vector is determined, it utilizes one of its optimization techniques to adjust the parameters to reduce the error function. ANFIS networks usually utilize a combination of least squares estimation and back propagation for membership function parameter estimation. The details of ANFIS structure can be found in [11]. Fig. 2(a) and 2(b) illustrates a generalized configuration and membership function for the proposed ANFIS network, respectively. The description of each layer in the ANFIS structure is explained in the following section.

Layer 1: The first layer is also known as the fuzzification layer, a number of membership functions are assigned to

$$x = \frac{\alpha - \alpha_{ref}}{\alpha_{rated}} \quad (1)$$

Here, $\alpha = \omega_r, V_{bus}$ or Q_s.

The membership functions are defined in this stage. The equations for the membership function are defined in (2)-(4).

$$\mu_{A1}^{1}(x) = \begin{cases} 1, & x \le b_1 \\ \frac{x-a_1}{b_1-a_1}, & b_1 < x < a_1 \\ 0, & x \ge a_1 \end{cases}$$

(2)

$$\mu_{A2}^{2}(x) = \begin{cases} 0, & |x| \ge b_2 \\ 1 - \frac{x-a_2}{b_2}, & |x| < b_2 \end{cases}$$

(3)

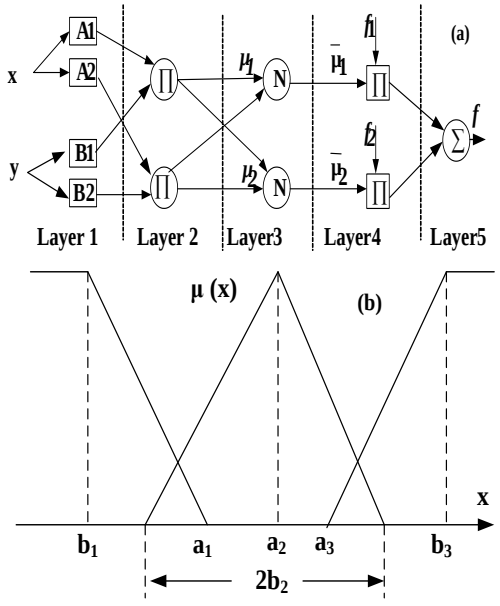

- Fig. 2: (a) Schematic of ANFIS architecture (b) Membership function for input data x.

$$\mu_{A3}^{3}(x) = \begin{cases} 0, & x \le a_3 \\ \frac{x-a_3}{b_3-a_3}, & a_3 < x < b_3 \\ 1, & x \ge b_3 \end{cases}$$

(4

Layer 2: In this layer, each node multiplies the entering signals and directs the output to the next level that represents the individual firing strength μi of a rule.

$$\mu_i = \mu_{A1}^{i}(x)\mu_{A2}^{i}(x)\mu_{A3}^{i}(x) \quad (5)$$

For the proposed controller only one input is chosen. So, the second layer can be ignored and the output of first layer goes to the third layer.

$$\mu_1 = \mu_{A1}^{1}(x), \mu_2 = \mu_{A2}^{2}(x), \mu_3 = \mu_{A3}^{3}(x)$$

(6)

Layer 3: Each block in the third layer which is also known as normalization stage, estimates the proportion of the i-th rule firing strength ($\bar{\mu}_i$) to the sum of the firing strength of all rules.

$$\bar{\mu}_i = \frac{\mu_i}{\mu_1+\mu_2+\mu_3} \quad (7)$$

Layer 4: In this layer, the function, fi is calculated as the linear activation function. A single input first order Sugeno fuzzy model is utilized in this model.

$$f_1 = \beta_0^1 + \beta_1^1 x \quad (8)$$

$$f_2 = \beta_0^2 + \beta_1^2 x \quad (9)$$

$$f_3 = \beta_0^3 + \beta_1^3 x \qquad (10)$$

In this stage, the parameters β_o, β_1 are tuned based on the operating condition of DFIG. These parameters are known as consequent parameters.

Layer 5: The final layer is the output layer which computes the overall output by combining the incoming data.

$$f = \bar{\mu}_1 f_1 + \bar{\mu}_2 f_2 + \bar{\mu}_3 f_3 \qquad (11)$$

2.2 Online self-tuning algorithm

It is impossible to calculate the desired outputs of the ANFIS controller, which are d-q axis currents for rotor and grid side control (idr, iqr, idg, iqg). Hence training data sequence can't be obtained especially for variable wind speed. Therefore, an unsupervised self-tuning algorithm is developed in the paper. The controller targets to minimize the objective function which is a squared normalized error function of the ANFIS controller input. The objective function is defined as,

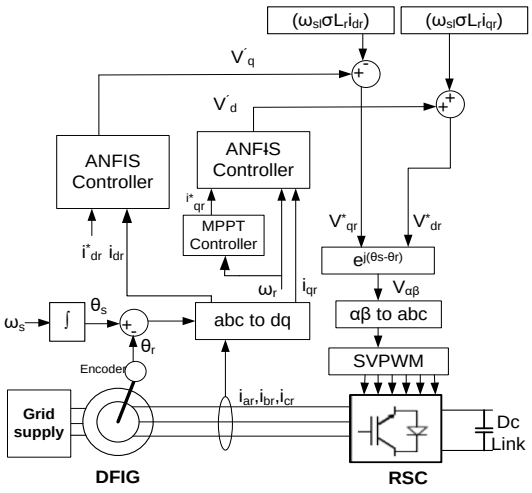

Fig. 3. ANFIS architecture based RSC control for grid-connected mode of DFIG

$$W = \frac{1}{2} e^2 = \frac{1}{2} \left(\frac{x^* - x}{x_{rated}}\right)^2 \qquad (12)$$

each input. Only one input is used in this layer which is the normalized error function of bus voltage (Vbus), rotor speed (ωr), reactive power (Qs) based on the converter control.

2.3 Tuning of Pre-Condition and Consequent

Parameters

The learning rule of the proposed controller can be given as [12]:

$$a_i(n+1) = a_i(n) - \gamma_{ai} \frac{\partial W}{\partial a_i}, \; b_i(n+1) = b_i(n) - \gamma_{bi} \frac{\partial W}{\partial b_i} \qquad (13)$$

Where, γ_{ai} and γ_{bi} are the learning rates of the corresponding parameters. The derivatives can be defined as:

$\frac{\partial W}{\partial a_i} = \frac{\partial W}{\partial e}\frac{\partial e}{\partial x}\frac{\partial x}{\partial f}\frac{\partial f}{\partial \mu_{Ai}^i}\frac{\partial \mu_{Ai}^i}{\partial a_i}$, $\frac{\partial W}{\partial b_i} = \frac{\partial W}{\partial e}\frac{\partial e}{\partial x}\frac{\partial x}{\partial f}\frac{\partial f}{\partial \mu_{Ai}^i}\frac{\partial \mu_{Ai}^i}{\partial b_i}$ (14)

Now we get, $\frac{\partial W}{\partial e} = e = \frac{x^* - x}{x_{rated}}, \frac{\partial e}{\partial x} = -\frac{1}{x_{rated}}$ and $\frac{\partial x}{\partial f} = J$, assuming J is the Jacobian matrix of the system. It is very difficult to determine system's Jacobian matrix. For decoupled control of DFIG, the system is assumed as a single input single output system and then the Jacobian matrix is considered as a positive constant. Considering that the effect of J is included in tuning rate parameter, the update rule for the consequent parameter is given as:

$a_1(n+1) = a_1(n) - \gamma_{a1} e(n) \frac{f_1(n)}{\sum \mu_{A1}^1} \frac{1-\mu_{A1}^1(n)}{b_1(n)-a_1(n)}$ (15)

$b_1(n+1) = b_1(n) - \gamma_{b1} e(n) \frac{f_1(n)}{\sum \mu_{A1}^1} \frac{\mu_{A1}^1(n)}{b_1(n)-a_1(n)}$ (16)

$b_2(n+1) = b_2(n) + \gamma_{b2} e(n) \frac{f_2(n)}{\sum \mu_{A2}^2} \frac{1-\mu_{A2}^2(n)}{b_2(n)}$ (17)

$a_3(n+1) = a_3(n) - \gamma_{a3} e(n) \frac{f_3(n)}{\sum \mu_{A3}^3} \frac{1-\mu_{A3}^3(n)}{b_3(n)-a_3(n)}$ (18)

$b_3(n+1) = b_3(n) - \gamma_{b3} e(n) \frac{f_3(n)}{\sum \mu_{A3}^3} \frac{\mu_{A3}^3(n)}{b_3(n)-a_3(n)}$ (19)

Similarly, the update laws for tuning the consequent parameters can be derived as follows.

$\beta_0^i(n+1) = \beta_0^i(n) - \gamma_{\beta_0^i} \frac{\partial W}{\partial \beta_0^i}$ (20)

$\beta_1^i(n+1) = \beta_1^i(n) - \gamma_{\beta_1^i} \frac{\partial W}{\partial \beta_1^i}$ (21)

$\gamma_{\beta_0^i}$ and $\gamma_{\beta_1^i}$ are the learning rates for the consequent $\beta_0^i(n+1) = \beta_0^i(n) - \gamma_{\beta_0^i} e(n) \frac{f_i(n)}{\sum \mu_{Ai}^i} \frac{\mu_i}{\mu_1+\mu_2+\mu_3}$ (17)

$\beta_1^i(n+1) = \beta_1^i(n) - \gamma_{\beta_1^i} e(n) \frac{f_i(n)}{\sum \mu_{Ai}^i} \frac{\mu_i x}{\mu_1+\mu_2+\mu_3}$ (18)

2.4 RSC Control by ANFIS Method

The rotor side converter magnetizes the machine through the rotor side converter. Fig. 3 shows the RSC control scheme using the proposed ANFIS architecture for grid connected DFIG.As DFIG provides decoupled control of real and reactive power, two different ANFIS structures have been employed to generate the reference d-axis and q-axis rotor voltages ($v_{dr}^* \; and \; v_{qr}^*$).

2.5 GSC Control by ANFIS Method

The grid side converter maintains the dc-link voltage constant irrespective of the value and direction of the rotor power flow. The ANFIS controller based configuration is implemented in GSC control to regulate

the dc-link voltage as depicted in Fig. 4. The reference q-axis grid current component can be obtained from the reactive power according to (19).

$$i_{qg}^{*} = K_Q Q_s^{*} = \frac{Q_s^{*}}{-3/2V_{grid}} \qquad (19)$$

The objective function of the ANFIS controller will ensure that the bus voltage error is converged to zero.

3. Performance Analysis of the Proposed Scheme

Speed and direction of wind at a location vary randomly with time. Therefore, the adaptability of controller is critical for wind power generators to operate effectively. ANFIS based controllers have the unique property of handling uncertainty and fast convergence in varying condition.

Table 1 Performance comparison among the proposed controllers

Operating condition	Property	PI controller	ANFIS based controller
Speed convergence characteristics	Speed settling time	Less than 0.2s	Less than 0.15s
	Speed overshoot	3.5%	0.6%
DC bus voltage convergence at variable wind flow	Voltage settling time	Less than 0.1s	Less than 0.05s
	Voltage fluctuation	Low	Very low
d-axis rotor current at step rise in reactive power demand	Current settling time	Less than 0.1s	Less than 0.2s
	Steady state error	Negligible	Higher steady state error
Computational burden	Block computation speed	Low	High
Ripple in grid currents at fixed wind speed		Low	High
Performance under Grid voltage disturbance		Good	Excellent

In this paper, the efficacy of the ANFIS controlled RSC for grid connected DFIG is observed under variable wind speed as shown in Fig. 5. The wind speed variation is depicted in Fig. 5(a).

It is found that the ANFIS controlled RSC tracks the rotor speed of the generator as dictated by the MPPT control algorithm (Fig. 5(b)). It also regulates the d-q axis rotor currents according to the demanded value to control the real and reactive power of the generator (Fig. 5(c,d)). Similarly,the GSC is controlled by the ANFIS based controller which regulates the d-q axis grid current components. The bus voltage regulation performance is depicted in Fig. 5(e). It is found that the ANFIS controller is capable to maintain the dc-link voltage to the reference set point which is 1150 V. A hysteresis current controller generates the control pulses for the grid converter. The current d-q axis grid current components and the three phase currents are shown in Fig. 5(f,g,h).

In DFIG, it is possible to control the reactive power requirement from RSC. Fig. 6 shows the feature for the proposed controller. The reference reactive power is varied from 0 to -0.5 MVAR by employing step function (Fig. 6(a)). The desired value of d-axis rotor current follows the variation of the reactive power and the actual

current component successfully can follow the trajectory of the reference current as observed in Fig. 6(b) and the three phase rotor currents also change accordingly (Fig. 6(c)). The reactive power regulation proves the accuracy and effectiveness of the ANFIS structure based controller in grid-connected DFIG based WECS.

To verify the competency of the proposed controller, the performance of the grid connected DFIG-WESC has been investigated for conventional PI and the proposed ANFIS based controller under various operating conditions. First, The dc-link voltage tracking performance between the controllers is compared and shown in Figs. 7(a)-(b). The voltage ripple and overshoot is relatively higher in constant gain PI controller compared to the ANFIS based NFC controller. The performance is also investigated for a step change in wind speed from 6 m/s to 8 m/s for each controller. The results are shown in Figs 7(c)-(d). It is observed from the figures that the ANFIS controller has the small overshoot but higher steady-state error compared to the PI controllers. Similarly, d-axis rotor current responses are investigated in Figs. 7(e-f) for a step change in reactive power demand. The PI controller shows fast current tracking while the NFC controller shows slightly improved performance in current tracking.

5. Conclusion

A novel ANFIS based NFC scheme for DFIG operated WECS has been presented in this paper. The performance of the proposed controller has been investigated for grid-connected machine under different dynamic operating conditions. The simulation results suggest that the RSC controller regulates the power by adjusting the rotor speed and machine torque with the variation of wind speed. Also, the GSC controller is capable of maintaining constant dc-link voltage and grid-current components even after abrupt variation of the required power demand and wind speed. The comparative analysis between the proposed scheme and conventional fixed-gain PI controller suggests the superiority and robustness of the ANFIS architecture based controller in power regulation of DFIG based WECS.

References

[1] Q. Wang & L. Chang, An intelligent maximum power extraction algorithm for inverter-based variable speed wind turbine systems, Transactions on Power Electronics, 19, 1242-1249, 2004.

[2] M.A. Abdullah, A.H.M. Yatim & C.W. Tan, An online optimum-relation-based maximum power point tracking algorithm for wind energy conversion system, Australasian Universities Power Engineering Conference (AUPEC), Australia, 1-6, 2014,

[3] H. Nian, P. Cheng & Z. Q. Zhu, Coordinated direct power control of DFIG system without phase-locked loop under unbalanced grid voltage conditions, IEEE Trans. on Power Electronics, 31, 2905-2917, 2016.

[4] M. K. Bourdoulis & A. T. Alexandridis, Direct power control of DFIG Wind systems based on nonlinear modeling and analysis, IEEE Journal of Emerging and Selected Topics in Power Electronics, 2, 764-775, 2014.

[5] M. E. Azzaoui, H. Mahmoudi & C. Ed-dahmani, "Backstepping control of a doubly fed induction generator integrated to wind power system", 2nd

International Conference on Electrical and Information Technologies (ICEIT), Tangiers, Morocco, 2016.

[6] P. Xiong and D. Sun, “Backstepping-based DPC strategy of a wind turbine-driven DFIG under normal and harmonic grid voltage”, IEEE Transaction on Power Electronics, vol. 31, pp. 4216-4225, June 2016.

[7] M. Azzouz,A.I. Elshafei and H. Emara“Evaluation of fuzzy-based maximum power-tracking in wind energy conversion systems”, IET Renewable Power Generation, vol. 5, pp.422-430, Nov. 2011 .

[8] S. Z. Chen, N. C. Cheung, K. C. Wong and J. Wu, “Integral sliding-mode direct torque control of doubly-fed induction generators under unbalanced grid voltage”, IEEE Transactions on Energy Conversion, vol. 25, pp. 356-368, June 2010.

[9] H. Li, K.L. Shi, P.G. McLaren, “Neural-network-based sensorless maximum wind energy capture with compensated power coefficient”, IEEE Transactions on Industry Applications, vol. 41, no. 6, Dec. 2005.

[10] H. M. Jabr, D. Lu and N. C. Kar, “Design and implementation of neuro-fuzzy vector control for wind-driven doubly-fed induction generator”, IEEE Transactions on Sustainable Energy, vol. 2, no. 4,pp. 404-413, October 2011.

[11] J.-S. R. Jang, C.-T. Sun, and E. Mizutani, Neuro-fuzzy and soft computing: a computational approach to learning and machine intelligence, Upper Saddle River, NJ: Prentice Hall, 1997.

[12] M.M.I. Chy, M.N. Uddin, “Development and implementation of a new adaptive intelligent speed controller for IPMSM drive” IEEE Transactions on Industry Applications”, vol. 45, no. 3, pp. 1106-115, May-June 2009.

[13] I.K. Amin, Robust Control Techniques for DFIG Driven WECS with Improved Efficiency, PhD dissertation, Dept. of Electrical Engineering, Lakehead University, Thunder Bay, ON, Canada, 2019.